

Experimental study of a reinforced concrete bridge pier strengthened with HPFRC jacketing

Adriano Reggia^{a,*}, Alessandro Morbi^b, Giovanni A. Plizzari^c

^a Department of Civil, Environmental, Architectural Engineering and Mathematics, University of Brescia, Brescia, Italy

^b Global Product Innovation, Heidelberg Cement Group, Bergamo, Italy

^c Department of Civil, Environmental, Architectural Engineering and Mathematics, University of Brescia, Brescia, Italy

ARTICLE INFO

Keywords:

Bridge pier
Structural rehabilitation
Seismic retrofitting
High performance fibre reinforced concrete
Jacketing

ABSTRACT

As a consequence of material degradation, increasing traffic loads and seismic actions, a large number of existing reinforced concrete bridges are no longer safe and may represent a risk for human lives and for the robustness of the road network. Replacement of these bridges is often not practical given the cost of demolition and rebuilding in addition to the social costs of traffic interruption. As an alternative to the replacement of the entire structure, the service life of a bridge can be extended by adopting reliable strengthening techniques. Among these strengthening techniques is High Performance Fibre Reinforced Concrete (HPFRC) jacketing, which was experimentally investigated in this research project. The mix design of HPFRC was studied with the goal of producing a material with enhanced mechanical performance as well as excellent rheology. In this study, the bridge pier studied was subjected to cyclic horizontal loads both before and after strengthening, up to failure. Experimental results show that the HPFRC jacketing remarkably increased the bearing capacity of the pier as well as its ductility. The jacketing also enhanced the structural response in terms of crack control, which significantly governs the structural durability.

1. Research significance

Prior to the introduction of modern design codes, the service life of reinforced concrete (RC) bridges was not always explicitly prescribed. Now, more than 50 years after the construction of large Reinforced Concrete (RC) infrastructures in many western countries, there is a major concern worldwide regarding their safety and their remaining service life due to material degradation, the increase of traffic loads and seismic risk. The bearing and deformation capacity of a RC bridge can be enhanced by means of various strengthening techniques. One of these techniques is High Performance Fibre Reinforced Concrete (HPFRC) jacketing, which provides improved resistance to environmental impact, thus increasing the service life of the infrastructure.

2. Introduction

Over the next few years, the number of Reinforced Concrete (RC) road infrastructures requiring repair or strengthening will rise in many Western countries since most of these infrastructures were built between the 50's and 70's in a completely different context in terms of traffic expectations and building codes. During the last 50 years, the

number of vehicles and the traffic loads have significantly increased; in addition, seismic regulations were introduced in structural codes and have been continuously updated. Furthermore, exposure to aggressive environments for several years has caused material degradation. For these reasons, there is an extreme need to verify and to restore the structural safety of road infrastructures and, especially, of bridges [1]. In Italy, the recent collapses of the “Annone” overpass, completed in 1962 in Annone Brianza, and the “Polcevera” Viaduct (i.e. “Morandi” Bridge), completed in 1967 in Genoa, are catastrophic examples of this need.

Regarding the effects of seismic action, which was often not considered at the time of bridge design, the main damages observed over the last 50 years are related to the bridge piers, where failure occurred due to a combination of shear and flexural actions (with possible overturning of the entire structure) [2].

A typical cross-section of bridge piers is the hollow rectangular cross-section whose seismic behaviour was investigated by Pinto and co-workers [3]. After testing pier specimens with constant axial load and horizontal cyclic load, a combined shear and bending failure, with the formation of the plastic hinges with inclined cracks, was observed.

Since seismic vulnerabilities of RC bridge piers are well known, a

* Corresponding author at: Via Branze, 43, 25123 Brescia, BS, Italy.

E-mail address: adriano.reggia@unibs.it (A. Reggia).

Table 1
Main design parameters of the critical cross-sections.

			Real scale	Reduced scale
Scale			(1:1)	(1:4)
Area of concrete	A_C	[mm ²]	9,385,960	596,250
Area of longitudinal reinforcement	A_S	[mm ²]	164,588	10,160
Longitudinal reinforcement ratio	ρ_S	[%]	1.75	1.70
Area of transverse reinforcement	A_{SW}	[mm ² /m]	12,060	3,060
Transverse reinforcement ratio	ρ_{SW}	[%]	0.20	0.20
Thickness of HPFRC	t_{HPFRC}	[mm]	120	30
Area of HPFRC	A_{HPFRC}	[mm ²]	1,963,200	113,100
Area of additional reinforcement	A_{S^*}	[mm ²]	47,008	2,941
Percentage of additional reinforcement	ρ_{S^*}	[%]	0.40	0.40
Axial load at the top of the column	N_{TOP}	[kN]	10,000	1,000
Axial load at the base of the column	N_{BOTTOM}	[kN]	17,500	1,100
Compressive stress at the base of the column	σ_C	[MPa]	1.48	1.47

number of retrofitting methods have been developed and studied over the last few years, namely: concrete jacketing, steel jacketing [4], or wrapping with fibre reinforced polymers (FRP) [5,6].

Concrete jacketing has become more efficient after the development of High Performance Fibre Reinforced Concrete (HPFRC). The bridge pier retrofitting with HPFRC jacketing [7] is hereafter considered, since this material combines a dense microstructure that ensures low porosity (and, thus, longer durability) than traditional concrete, in addition to a higher compressive (generally more than 100 MPa) and tensile strength (over 10 MPa), that guarantee satisfactory structural performance.

The experimental study on mechanical properties of the HPFRC selected for this research was initially carried out by Cangiano and co-workers [8] by testing cylinders of normal strength concrete (NSC) with a diameter of 100 mm and a height of 300 mm, coated with a 25 mm HPFRC jacketing. Samples subjected to compression showed an increased resistance of about 60%, with a controlled failure mechanism due to the presence of steel fibres in HPFRC.

Similar results were found by Gholampour and co-workers [9] on NSC cylinders with a diameter of 100 mm and a depth of 200 mm, coated with 25 mm of different repair materials containing polyethylene fibres. An increase of load bearing capacity (in compression) and ductility was observed in FRC specimens containing traditional steel reinforcement (stirrups), while specimens with no fibres or stirrups showed a brittle failure with a rapid loss of strength after peak.

The idea of strengthening deteriorated concrete structures with HPFRC layers was deeply investigated by Brühwiler and co-workers [10] both for bridge decks [11] and piers [12]. The application of a 40 mm HPFRC overlay on the deck slab of the Chillon viaduct in Switzerland aimed at increasing slab resistance, stiffness and durability. Another application concerned a motorway bridge in Switzerland with the use of 40 mm thick pre-fabricated HPFRC shell elements, applied around a deteriorated pier in order to improve durability and strength.

A similar solution was experimentally studied by Ilki and co-workers [13] using HPFRC pre-fabricated panels (30 mm thick) to strengthen columns made of low-strength concrete or with a short lap splice length of longitudinal reinforcement. Experimental results showed an increase of the strength and deformation capacity, even though a concentration of damage at the interface between the joint and the column was observed.

Experimental tests on HPFRC jacketing were carried out by Meda and co-workers [14] on RC columns where longitudinal reinforcing bars were subjected to artificial corrosion. A 40 mm thick HPFRC jacketing was applied to the columns after removing the oxidation products from the reinforcing bars and sandblasting of the surface of the column. The experimental response of the reinforced columns showed an increase of the lateral load and ductility, even though cracks localized at the interface between the foundation and the jacketing itself. Similar tests were carried out by Marini and co-workers [15] on RC shear walls.

Experimental tests on RC columns strengthened with sprayed

HPFRC were performed by Cho and co-workers [16]. HPFRC was applied on the previously grooved surface of the existing columns. Additional reinforcing bars, both transverse and longitudinal, were added to the specimens. The proposed strengthening method was sufficient to enhance the load-carrying and deformation capacity of the structure by limiting shear and bending cracks in the region of the plastic hinge.

Local HPFRC repair of large scale bridge pier specimens built according to the code requirements used prior the 70's was investigated by Dagenais and co-workers [17]. Critical lap splice zones at the base of the bridge piers were effectively strengthened by removing the existing concrete cover and replacing it with a new layer of HPFRC. Retrofitted specimens were able to sustain several cycles of lateral loading and to reach high ductility without buckling of longitudinal bars.

The aim of the present paper is to study the seismic response of an existing RC bridge pier (having a hollow cross section) after HPFRC jacketing. Referring to a real bridge as a case study, the seismic response of a large scale specimen, strengthened with a thin layer (30 mm) of HPFRC, was experimentally investigated by means of a cyclic test. Experimental results concerning the lateral load-drift response, the moment-curvature behaviour, and the crack pattern development are carefully described and discussed to assess the effectiveness of the proposed strengthening technique.

3. Case study

The structure under investigation is a real highway bridge with a 23 m tall pier supporting three 50 m single-span prestressed concrete box girders, having a depth of 2 m. The deck was made of a reinforced concrete slab 14 m wide and 0.15 m thick. The bridge pier had a hollow cross-section with external dimensions of 6 × 2.5 m and two internal cells of 2.1 × 1.3 m. At the base section, the pier was reinforced by 314 Ø26 longitudinal bars and Ø16 transverse reinforcements spaced 100 mm, with a concrete cover of 40 mm. Table 1 summarizes the main geometrical characteristics of the cross-section. Typical materials of the 60's, namely C30/37 concrete and high ductility steel rebars (very similar to B450C), were adopted for the construction of the bridge. The axial load at the top of the pier in seismic loading conditions (considering dead loads and factorized live loads) was about 10,000 kN, while the axial load at the base of the pier (including the self-weight) was about 17,500 kN.

4. Experimental investigation

4.1. Strengthening design of the existing bridge pier

The design of the seismic retrofitting was performed in order to increase service life of the existing structure from 50 to 100 years, as required by modern building codes. Seismic actions were calculated by increasing the peak ground acceleration from 0.250g (related to a

nominal life of 50 years) to 0.309-g (related to a nominal life of 100 years) for a high seismicity location in Italy. In addition to the seismic retrofitting, the jacketing herein presented also aims at enhancing structural durability.

Structural performance was increased by the enhanced compressive strength and toughness of HPFRC as well as by rebars. The use of traditional steel rebars was limited to zones with the highest bending moment (such as the base of the bridge pier); in the remaining areas of the bridge pier, only the HPFRC jacketing was adopted. The bridge pier was sufficiently slender ($H/d \approx 10$) to be considered more vulnerable to flexural actions than to shear actions. In fact, the shear strength of the existing structure was considered adequate to meet the new code requirements; therefore, the contribution to the shear strength of the HPFRC jacketing, which can also be considered as significant given the material performance, was neglected in the retrofitting design. In particular, the flexural capacity of the existing structure was increased by the larger internal lever arm as well as by the enhanced tensile strength in the cracked area (due to the post-cracking strength of HPFRC).

The structural durability is enhanced by the low porosity of the high-performance cement matrix as well as by the higher toughness of fibre-reinforced concrete that limits the crack openings, thus providing a better protection against the aggressive agents present in the environment [18].

4.2. Specimen description

The test specimen adopted was a 1:4 scale reproduction of the bridge pier described in Section 3; however, it is also representative of a medium-size bridge. The choice of the scale was influenced by several factors, including the size of the specimen allowed by the laboratory facilities (i.e. the height of the reaction wall (8 m), the capacity of the reaction wall (1000 kN)), as well as the stiffness of the strong floor to which the specimen was anchored (i.e. a RC floor 1 m deep). Another important factor was the thickness of the jacketing to be successfully applied to the specimen by pouring HPFRC in formworks (a minimum thickness of 25 mm was considered viable). A further factor was to have specimen dimensions significant for many existing bridges, in order to consider the experimental pier as a full-scale specimen.

For all of the above reasons, the test specimen was a 7 m high column, having a cross-section of 1.50×0.62 m with two internal cells (0.53×0.32 m) along the whole specimen depth (see Fig. 1). The wall thickness of the hollow cross section was 0.15 m. The reinforcement consisted of 66 $\varnothing 14$ longitudinal bars and $\varnothing 8$ transverse reinforcements spaced at 100 mm, with a concrete cover of 10 mm. The cross-section area was equal to $596,250 \text{ mm}^2$ and the total longitudinal reinforcement area was $10,160 \text{ mm}^2$, corresponding to a reinforcement ratio of

1.70%, as in the real bridge.

The jacketing layer of HPFRC was 30 mm thick. Additional reinforcement was provided to connect the HPFRC jacketing to the foundation at the base of the pier. The additional reinforcement was designed to yield when the HPFRC reached its tensile strength, thus providing additional ductility to the section. The additional reinforcement consisted of $(13 + 13) \varnothing 12$ longitudinal bars (spaced at 100 mm), with a concrete cover of 10 mm. Table 1 summarizes the main geometrical characteristics of the cross-section as compared to the real one.

The additional rebars were extended along the critical zone (corresponding to $1/3$ of the height of the pier) and, then, post-installed in the foundation with epoxy resin anchors 0.25 m long. The reinforcement ratio, considering both the existing concrete element and the new reinforcing layer, was equal to 2.10%. Cold joints were locally reinforced with $(13 + 13) \varnothing 12$ longitudinal bars 300 mm long, placed across the cold joint.

The interface between the jacketing layer and the existing concrete was tested before the full-scale test with several local bond tests to verify bond strength at the interface; these tests demonstrated that sandblasting was sufficient (and steel connectors were not necessary) for guaranteeing a good bond behaviour.

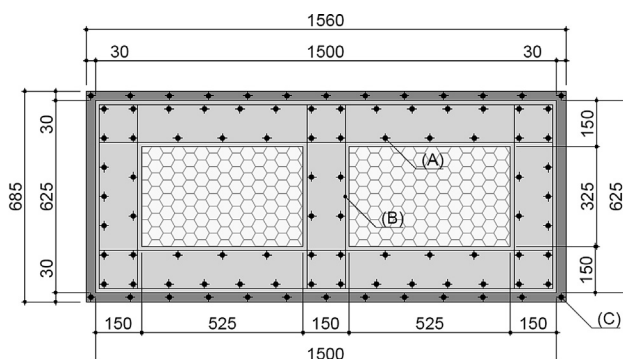
4.3. Materials properties

The existing pier was made of Normal Strength Concrete (NSC) with cement CEM II/A LL 32.5 R and a water/cement ratio 0.45. Workability class S5 was obtained with the use of Superplasticizer (SP). The maximum aggregate size was 10 mm.

The external jacketing was made of self-compacting HPFRC with 565 kg/m^3 of cement CEM I 52.5R and a water/binder ratio equal to 0.22 with 272 kg/m^3 of slag. Admixtures were also adopted in HPFRC, namely Superplasticizer (SP, 8 kg/m^3) and Shrinkage Reducing Admixture (SRA, 8 kg/m^3). Stainless steel fibres, with a volume fraction of 1%, were included in HPFRC. Fibres were crimped, 19 mm long, with a diameter of 0.13 mm, thus having an aspect ratio of 1:146. Basaltic sand (1461 kg/m^3) with a maximum aggregate size of 4 mm (to fit the low thickness – 30 mm – of the jacketing) was adopted. The composition of HPFRC was chosen in order to obtain a compromise between performance, cost and easy handling on the construction site; it was optimized on the basis of the final application by passing through an iterative path. Silica fume was avoided because its handling on a construction site is difficult and because of its risk for human health. The composition of HPFRC is reported in Table 2.

Hardened properties of NSC and HPFRC were experimentally determined according to the following Standards: EN 12390-3 for cubic compressive strength, EN 12390-6 for indirect tensile strength, EN 12390-13 for elastic modulus and EN 14651 for fracture toughness (flexural residual strengths). Table 3 summarizes all the experimental results.

Compressive strength of NSC was measured after 28 days, after 210 days (at the beginning of the test of the un-strengthened specimen), and after 270 days (at the beginning of the test of the strengthened specimen) of curing; it was found to be 42.5 MPa, 48.4 MPa, and



- (A) Longitudinal reinforcement 66 $\varnothing 14$
- (B) Transverse reinforcements $\varnothing 8 @ 100 \text{ mm}$
- (C) Additional reinforcement $(13+13) \varnothing 12$

Fig. 1. Critical (base) section of the strengthened specimen (measures in millimetres).

Table 2
HPFRC composition.

		HPFRC
Cement CEM I 52.5 R	[kg/m^3]	565
Aggregates	[kg/m^3]	1461
Pozzolanic addition	[kg/m^3]	272
SP admixture	[kg/m^3]	8
SRA admixture	[kg/m^3]	8
Steel fibres	[kg/m^3]	78
Water/binder ratio	[-]	0.22
Maximum aggregate size	[mm]	4

Table 3
Mechanical properties of NSC and HPFRC: number of tests (n), mean value (μ), standard deviation (σ), and coefficient of variation (CoV).

Age from casting	[days]	NSC			HPFRC
		28	210 (First test)	270 (Second test)	28 (Second test)
Compressive strength	n [-]	3	3	3	12
	μ [MPa]	42.5	48.4	49.4	136.3
	σ [MPa]	2.5	2.6	3.6	3.0
	CoV [-]	6%	5%	7%	2%
Indirect tensile strength	n [-]	–	3	3	12
	μ [MPa]	–	3.4	4.6	14.1
	σ [MPa]	–	0.6	0.6	3.1
	CoV [-]	–	17%	13%	22%
Modulus of elasticity	n [-]	–	3	3	3
	μ [MPa]	–	34,510	36,035	44,879
	σ [MPa]	–	1249	4838	1048
	CoV [-]	–	4%	13%	2%
Residual tensile strengths	$f_{l,OP}$ [MPa]	–	–	–	10.6
	f_{R1} [MPa]	–	–	–	10.4
	f_{R2} [MPa]	–	–	–	8.9
	f_{R3} [MPa]	–	–	–	6.9
	f_{R4} [MPa]	–	–	–	5.5

49.5 MPa, respectively. Therefore, the concrete class can be assumed as C30/37. Indirect tensile strength was measured after 210 days and 270 days, obtaining values of 3.4 MPa and 3.5 MPa, respectively. Modulus of elasticity was measured at the same stages, obtaining values of 34,510 MPa and 36,035 MPa, respectively.

All tests on HPFRC were carried out after 28 days of curing (corresponding to the beginning of the test of the strengthened specimen); it should be noted that the compressive strength of HPFRC was 136.3 MPa. Significant values (from flexural tests according to EN 14651) for SLS (f_{R1}) and for ULS (f_{R3}) were 10.4 MPa and 6.9 MPa, respectively. According to the Model Code 2010 [19], post-cracking strength class of HPFRC was 5a.

Uniaxial tensile tests were also carried out on dog bone specimens; typical experimental results are shown in Fig. 2. The mean value of the maximum (peak) tensile stress was 4.5 MPa while the mean value of the deformation at peak stress was 0.035%.

Hot rolled B450C rebars, having similar properties of FeB44k rebars, were used as reinforcement.

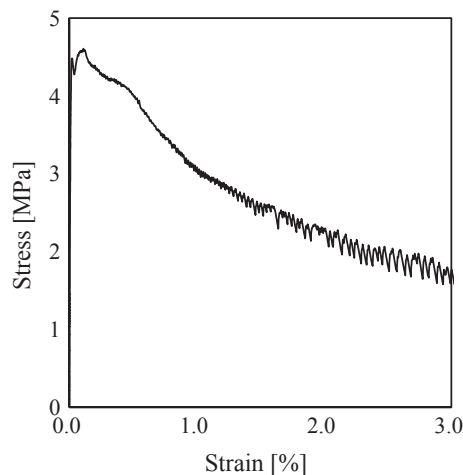


Fig. 2. Typical Stress vs. deformation curve from uniaxial tensile tests on dog-bone specimens.

4.4. Experimental program

The experimental program was characterized by the following phases:

1. **Specimen preparation.** The existing bridge pier was cast with ready-mix concrete in a horizontal position to avoid cold joints. The internal cells were produced by means of expanded polystyrene blocks placed inside the reinforcement cages.
2. **Un-strengthened specimen test.** The first test was performed on the un-strengthened specimen (210 days after casting), under a constant axial load of 1,000 kN (causing the same compressive stress of the existing pier in the base section, as described in Table 1) and a cyclic horizontal load up to a value of 100 kN. This load level was selected to simulate the service conditions of the structure, assumed as 50% of the theoretical load causing yielding in the reinforcements.
3. **Surface preparation.** After the first test, the lateral surface of the specimen was sandblasted to obtain a very rough surface ($R_t = 3.0$ mm), measured with sand patch method [19]. After sandblasting, the lateral surface was cleaned with air pressure. Prior to the application of HPFRC, the lateral surface was pre-wetted until reaching saturated surface dry (SSD) condition.
4. **Jacketing application.** HPFRC pouring was performed in four phases using light weight climbing formworks. The formwork system consisted of panels and external steel ties to counteract the pressure of fresh HPFRC. The latter was made with a planetary mixer (available in the laboratory) with a capacity of 250 L. Rheology of the material was appropriate to fill the formworks from a height of 1.80 m. HPFRC was applied with axial load acting on the existing pier to better simulate the application on a real structure, where dead loads cannot be removed. After formworks removal, the surface of HPFRC was water-cured for 24 h and covered with polyethylene film up to the following phase.
5. **Strengthened specimen test.** The second test was carried out under a constant axial load of 1,000 kN and an increasing cyclic horizontal load up to failure. The test was performed after 28 days of HPFRC curing (270 days after casting NSC).

4.5. Test setup

The test setup is shown in Fig. 3 and Fig. 4. The axial load (1,000 kN) was applied with two hydraulic jacks, arranged symmetrically on both sides of the specimen, through two high-strength steel post-tensioning bars. The hydraulic jacks were placed above a steel beam (2 UPN400), placed on the top of the pier. Vertical bars were anchored to the reaction floor by means of hinged supports. The set-up for vertical loading allowed monitoring of the top displacement of the specimen during the application of the horizontal loading. However, given the simplicity of the test set-up, for large horizontal displacements the elongation of the vertical bars provoked an increment of axial load and a horizontal component contrasting with the applied horizontal load. Therefore, the vertical load was corrected every cycle by the reduction of the pressure in the vertical jacks for increasing displacements, then progressively restored when the specimen was approaching the vertical position. The horizontal load was corrected by considering the horizontal component provided by the post-tensioned rebars.

The cyclic horizontal load was applied by means of an electro-mechanical actuator with a maximum capacity of 1,500 kN. Two steel beams (UPN400) were adopted to distribute the load over the specimen width. The set-up for horizontal loading allowed to apply both traction and compression. The maximum possible displacement of the horizontal screw jack was 250 mm in both directions. The horizontal load was applied under displacement control in quasi-static conditions with a maximum speed (for larger cycles) of 2 mm/min.

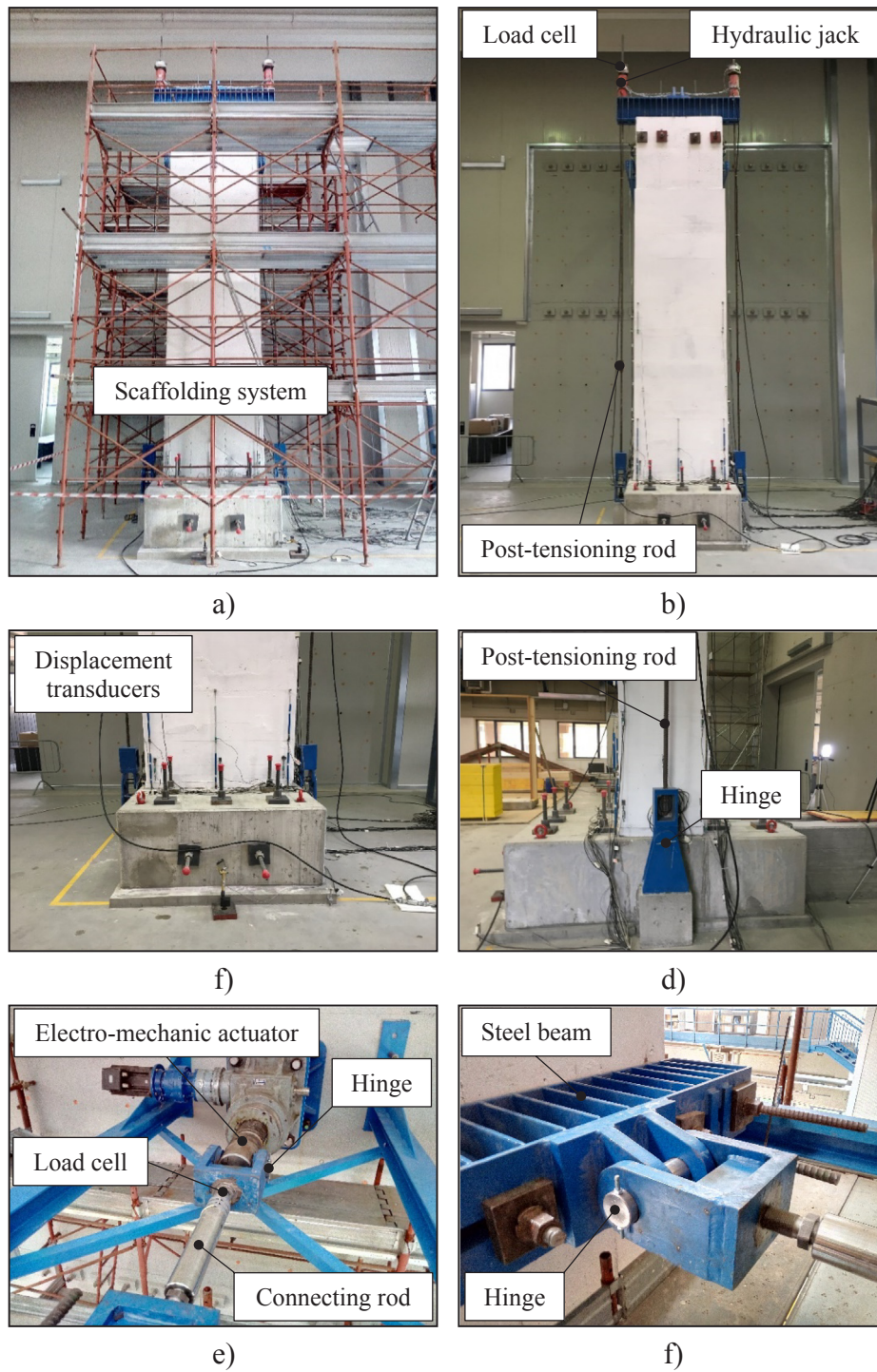


Fig. 3. Pictures of the test setup: test of the un-strengthened specimen (a), test of the strengthened specimen (b), specimen foundation front view (c) and side view (d), horizontal loading system connected with the reaction wall (e) and to the specimen (f).

4.6. Loading protocol

The test on the un-strengthened specimen was carried out up to a drift of 0.2%, representing service conditions, while the test on the strengthened specimen was carried out until failure under cyclic loads by increasing the drift according to the test protocol reported in Fig. 5. Every set of cycles was repeated three times, with exception of the last two cycles. The drift (θ) was defined as the ratio between the lateral displacement at the horizontal load point and the distance between the load point and the base of the pier.

4.7. Instrumentation

A number of different measuring devices were adopted for the tests, as described in the following and represented in Fig. 6. One load cell, with a maximum capacity of 500 kN, was mounted on the connecting rod to measure horizontal load. Two load cells, with a maximum capacity of 1,000 kN each, were positioned above the two hydraulic jacks to measure axial load in each vertical bar.

Displacement transducers were used to:

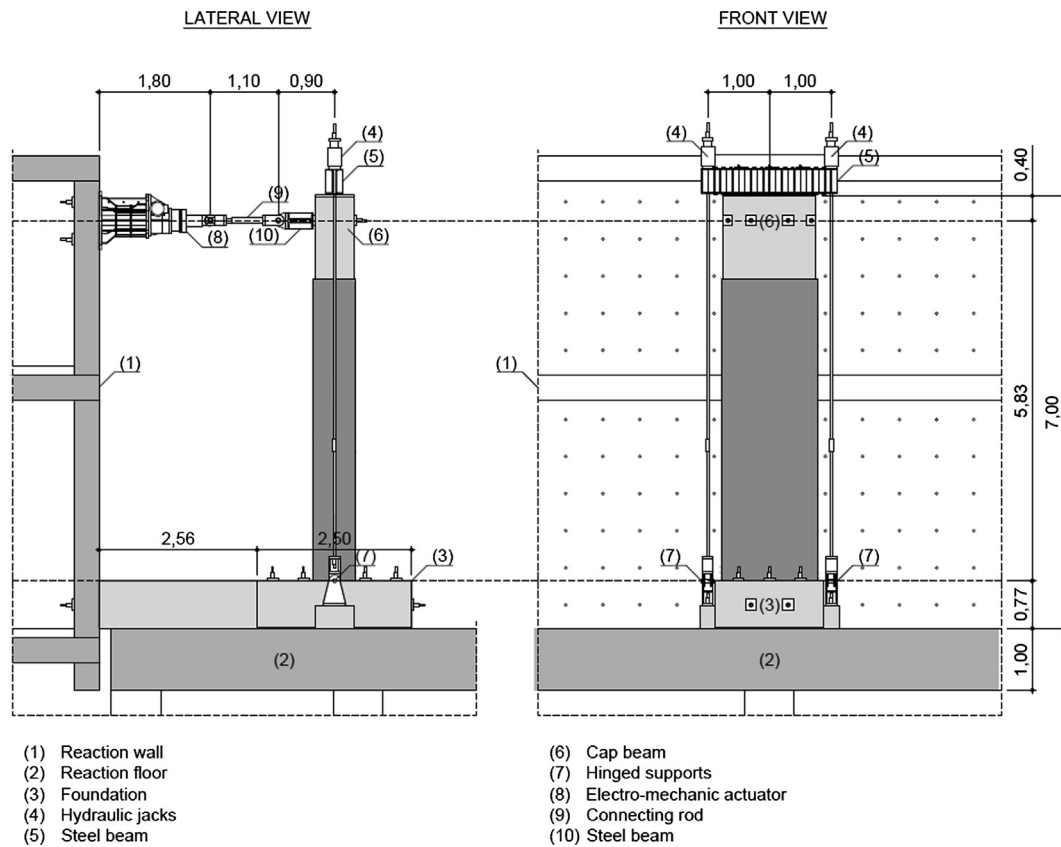


Fig. 4. Test setup (measures in metres).

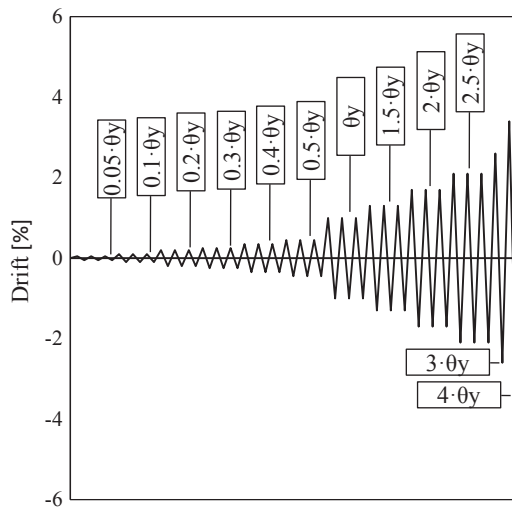


Fig. 5. Horizontal-loading cycles ($\theta_y = 0.8\%$).

- monitor horizontal and vertical displacements on both sides of the load point;
- monitor rotation and rigid translation of the foundation;
- measure deformation/crack openings on front and back sides of the specimen in the zone of the formation of the plastic hinge, and
- measure the curvature of some sections in the bottom part of the specimen.

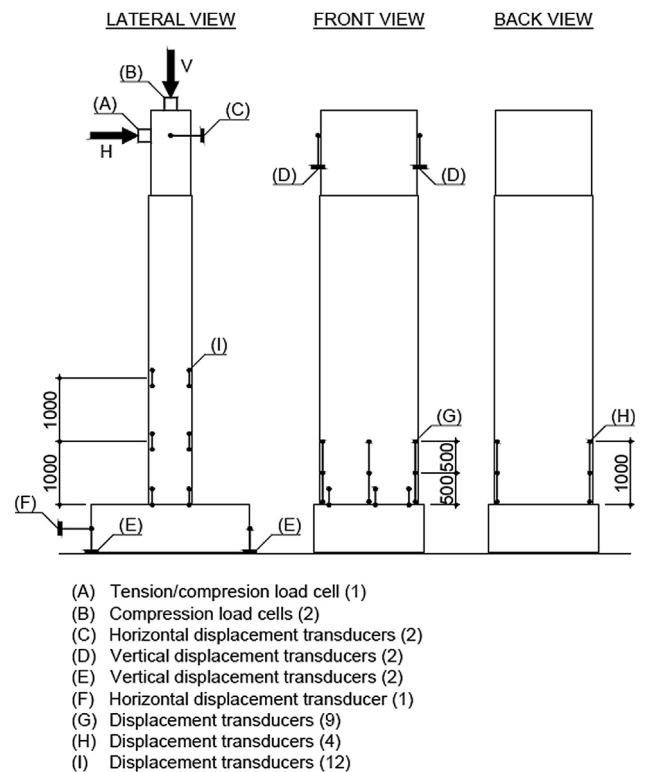


Fig. 6. Instrumentation adopted during testing of the strengthened specimen.

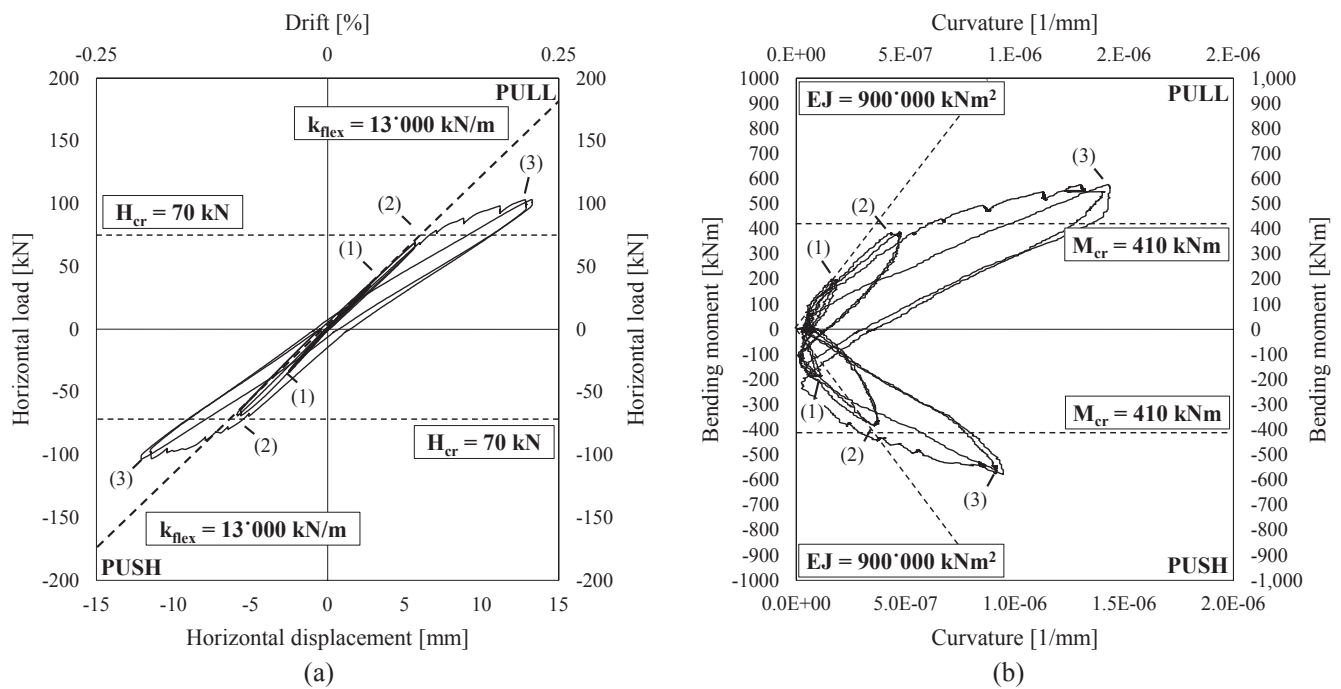


Fig. 7. Horizontal load vs. horizontal displacement (a) and Bending moment vs. Curvature (b) of the un-strengthened specimen.

5. Experimental results

5.1. Un-strengthened specimen

Fig. 7a shows the seismic response of the un-strengthened specimen (positive displacements are toward the strong wall) where the load takes into account the horizontal component of the post-tensioned rebars for the axial load.

As mentioned above, the un-strengthened specimen was tested up to a drift of 0.2%, resulting in a maximum horizontal load of 100 kN on both sides. Fig. 7a clearly shows that, in the first phase, the lateral response of the structure was linear, with a stiffness of 13,000 kN/m (very close to the theoretical value of 14,000 kN/m), obtained by considering both bending and shear deformability of the element.

The diagram of bending moment versus curvature of the base section is shown in Fig. 7b. During cycles at 0.05% and 0.1% drift, the slope of the curve (EJ) can be estimated as 900,000 kNm², similar to the theoretical value of 940,000 kNm². During the first cycle at 0.2% drift, the slope of the curve clearly changes after first cracking (410 kNm). The following two cycles at 0.2% drift have a reduced stiffness due to the cracked state of the element.

5.2. Strengthened specimen

The experimental response of the strengthened specimen is shown in Fig. 8a (results are presented with the same diagrams of the un-strengthened specimen). In the first phase, during cycles at 0.05% and 0.1%, the lateral response was linear, with a lateral stiffness of about 20,000 kN/m; therefore, an increment of stiffness (+54%) of the strengthened specimen, with respect to the un-strengthened one, can be observed.

The first cracking of the HPRFC jacketing was observed with a horizontal load equal to 100 kN (corresponding to the tensile strength experimentally obtained for HPRFC), with an increment of +43% as compared to the un-strengthened pier.

In the following cycles, lateral stiffness of the strengthened element continued decreasing due to the combined effect of cracks, developed in most parts of the element, and yielding of reinforcements in the critical

section, developing in the plastic hinge at the base of the element. The specimen reached a maximum load of 406 kN with a drift of 3.4%.

While in positive direction the lateral load continued increasing up to the end of the test, in the negative direction the resistance reached a maximum value of 376 kN during the cycle with a drift of 1.70%, followed by a decreasing branch. Pier collapse occurred for buckling of the rebars at the base of the pier. After the local delamination of the jacketing (due to rebar buckling), the test was interrupted to avoid any possible dangerous failure of the element. The moment–curvature curve of the strengthened specimen is shown in Fig. 8b; it can be observed that the slope of the curve remained constant up to a drift of 1.3%, in both directions. The initial stiffness (EJ) was about 70% higher than the un-strengthened specimen; Fig. 8c shows the stiffness degradation vs. drift.

Numerous techniques and models are available in the literature for calculating plastic hinge length; an equivalent plastic hinge length l_p is herein adopted, as proposed by Pauley and Priestley [20]: over the length l_p the plastic curvature (ϕ_p) is assumed equal to the maximum plastic curvature ($\phi_m - \phi_y$). Fig. 8d shows the moment–curvature curves measured in three different sections along the height of the element, in particular at 0, 500 and 1,000 mm from the base. While the section at the base is characterized by a complete development of the plastic curvature (about 0.000070 mm⁻¹), the section at 1,000 mm is near the yielding point (about 0.000006 mm⁻¹). On the basis of this observation, it can be assumed that the distribution of plastic curvature (ϕ_p) varies between zero (in the section at 1,000 mm) and the maximum ($\phi_m - \phi_y$, at the base section) proportionally to the bending moment (which varies linearly). It is therefore reasonable to assume that the length of the plastic hinge is about half of the of the plasticity length, corresponding to about 500 mm. The calculated value of equivalent plastic hinge length from experimental measures of cantilever top displacement according to the procedure proposed by Pauley and Priestley [20], is equal to is 490 mm, by considering a plastic displacement of 175 mm. The calculated value of equivalent plastic hinge length from Paulay and Priestley [20] is 629 mm. Because of the overall good agreement between values predicted and experimental observations, it can be assumed that the effect of post tensioning of steel bars for applying the axial force to the pier does not substantially alter

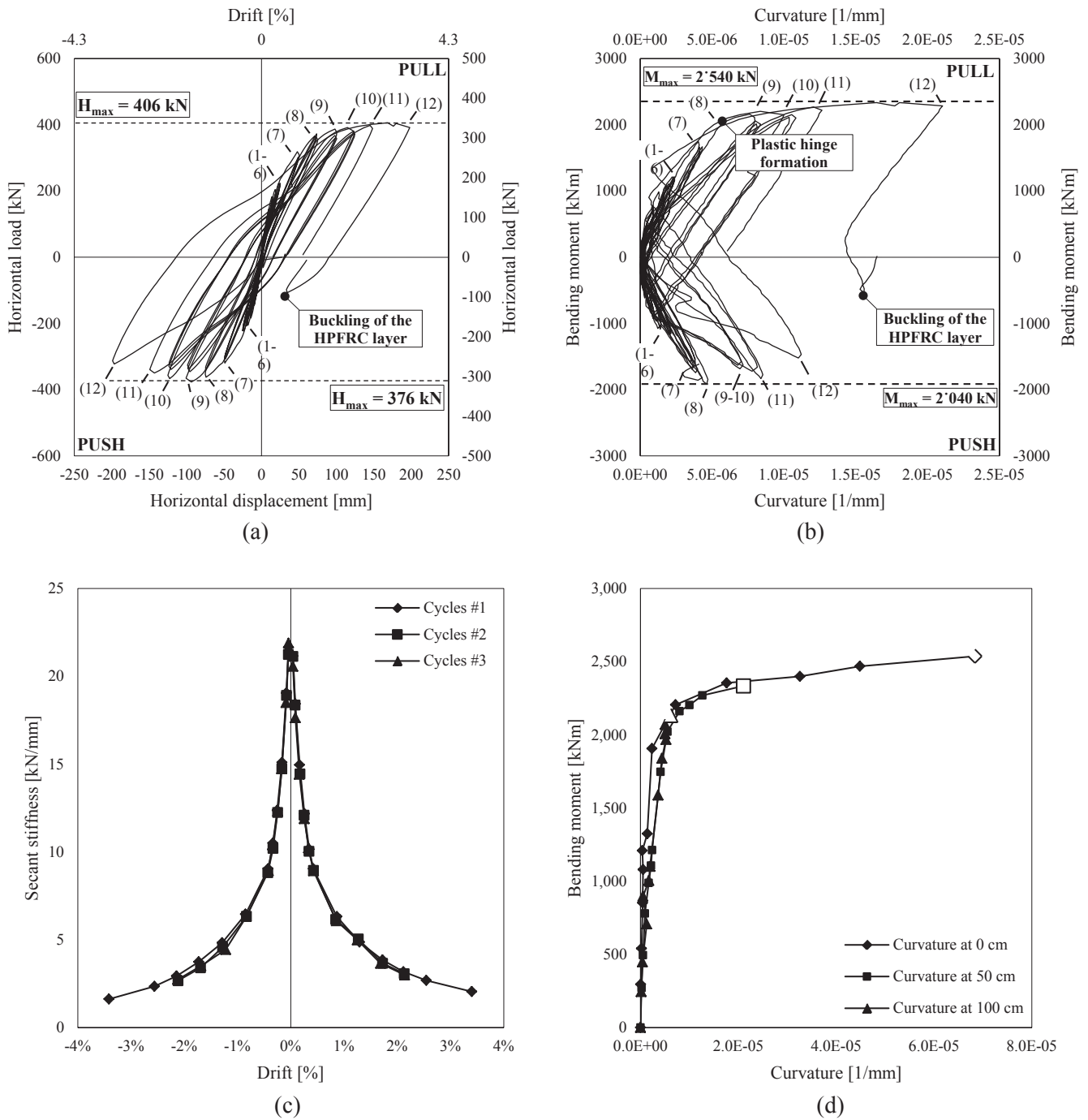


Fig. 8. Horizontal load vs. horizontal displacement (a), bending moment vs. curvature at the base section (b), stiffness degradation vs. drift (c) and bending moment vs. maximum curvatures at different sections (d).

the development of the plastic hinge. However, it can be emphasized that the analytical formulations available in the literature, developed for traditional RC, should be better calibrated for high performance concrete, used both for new structures and for the retrofitting of existing ones.

Experimental ductility in terms of curvature was around 6 in the un-strengthened specimen and increased to 14 in the strengthened one while the displacement ductility increased from 2 (in the un-strengthened specimen) to 3.6 (in the strengthened specimen).

Fig. 9 shows the experimental total dissipated energy, as the sum of the areas enclosed in each hysteretic loop vs. the drift.

5.3. Cracking and failure

Visual inspection of the crack development was carried out on the four faces of the specimen at various drift steps. Fig. 10 shows the crack patterns on the south (front) face for drift values equal to 0.25%, 1.7% and 3.4%. It can be observed that the HPFRC allows an excellent crack control; first cracks near to the base of the element were observed for a drift of 0.1%, with an average crack width of 0.078 mm.

Splitting cracks along the rebars were observed for a drift of 0.25%; at the same drift level, the opening of the cold joint (at the pier base) was observed (anyhow limited by local reinforcement). At 1% drift, the average crack width was 0.190 mm and the average crack spacing was 83 mm. For drift values higher than 1.70%, no additional cracks

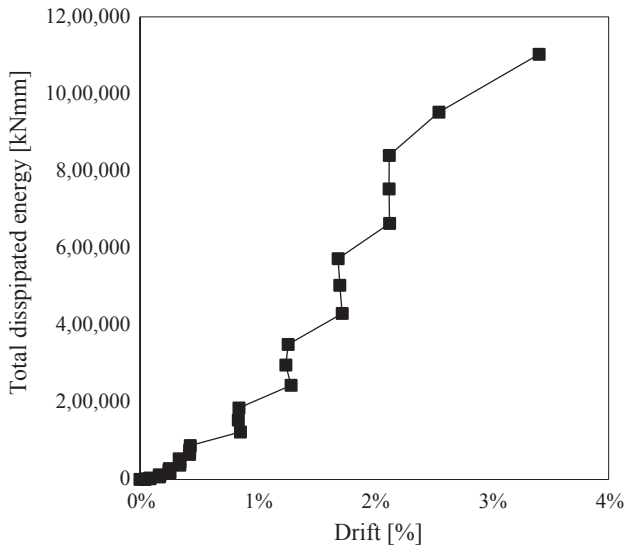


Fig. 9. Total dissipated energy vs. drift.

formed, but those already present became larger due to the rebar yielding with a visible damage accumulation.

At the end of the test, the average maximum crack width was 0.683 mm and the average crack spacing was around 85 mm. No spalling, exposure or fracture of reinforcements were observed at the end of the test.

5.4. Comparison between the response before and after jacking

The structural response at ULS of the un-strengthened specimen was determined by means of the classical sectional theory. The load-displacement curve of the un-strengthened specimen (Fig. 11) was

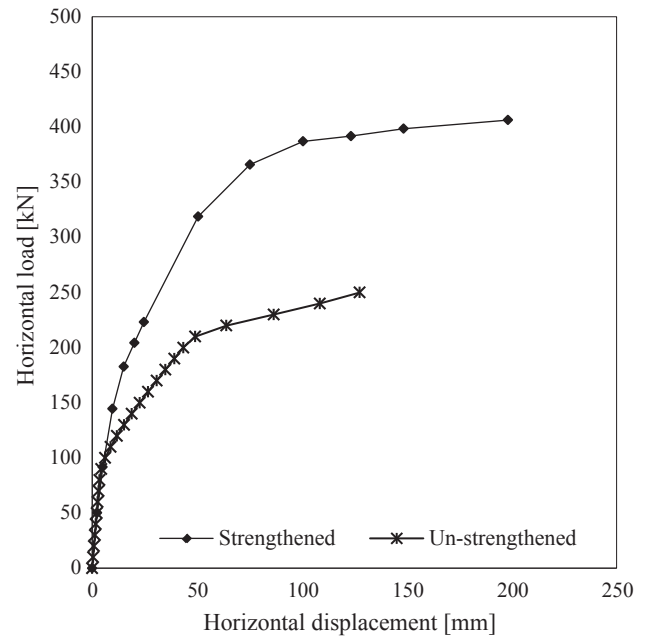


Fig. 11. Comparison between the structural response of the strengthened specimen (envelope of the response curve) and the un-strengthened specimen.

calculated considering the specimen deforming as a cantilever (fixed at the base), under a constant vertical load and an increasing horizontal load acting on the top of the element. The non-linear response of the element was predicted by progressively increasing the horizontal load and calculating the corresponding horizontal displacement by integration of the curvature of each section of the element. Bending moment was calculated by considering geometrical non-linearities due to the

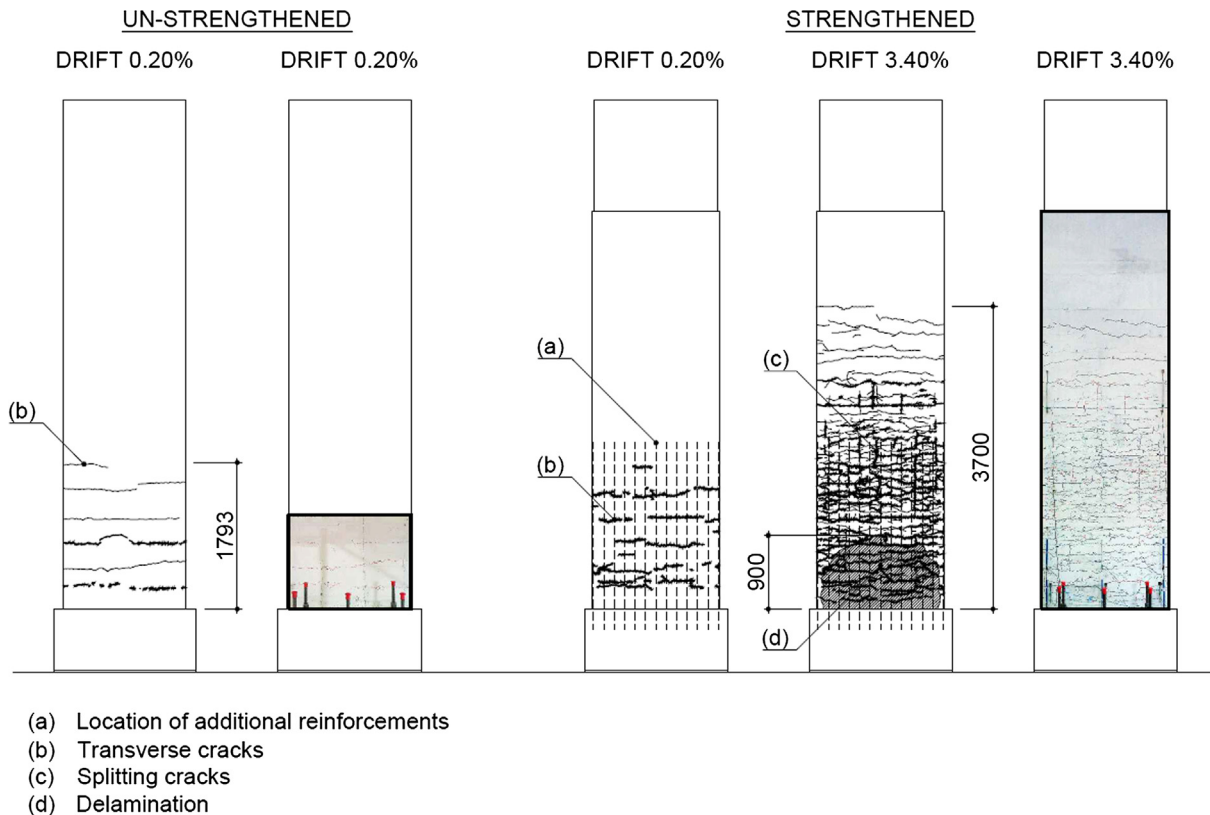


Fig. 10. Crack pattern of the strengthened specimen: front face (measures in millimetres).

Table 4

Comparison between the main results obtained from the pier before and after the application of the HPFRC jacketing: maximum horizontal force (H), maximum horizontal displacement (d), and maximum drift (θ).

		Units	Un-strengthened	PUSH Strengthened	Variation	PULL Strengthened	Variation
First cracking	H	[kN]	70	100	(+42%)	100	(+42%)
	θ	[%]	0.1	0.1	(-14%)	0.1	(-14%)
Yielding	H	[kN]	208*	366	(+76%)	362	(+74%)
	θ	[%]	0.8*	1.2	(+50%)	1.2	(+50%)
Failure	H	[kN]	259*	406	(+57%)	322	(+24%)
	θ	[%]	2.1*	3.4	(+57%)	3.4	(+57%)

* Calculated values with $f_y = 450$ MPa.

relative displacement of the vertical load with respect to the base. The bending moment–curvature relationship was calculated considering non-linear behaviour of concrete and steel.

The experimental response of the strengthened specimen shows a higher maximum load and maximum drift with respect to the un-strengthened specimen. In particular, with respect to the predicted behaviour of the un-strengthened specimen, the flexural capacity of the strengthened pier increased up to 57%. The increment of load bearing capacity was provided by the additional reinforcement, by the post-cracking tensile strength of HPFRC, and by the increased lever arm of internal forces generated by the high compressive strength of HPFRC.

The load related to first cracking and yielding of steel reinforcements increased up to 42% and 76%, with respect to the theoretical prediction. The comparison of maximum displacement is not possible since the experimental measurements for the un-strengthened specimen are not available. Table 4 summarizes the enhancement in terms of maximum horizontal force (H) and maximum drift (θ).

Failure of the strengthened specimen, due to buckling of the HPFRC layer, caused the delamination of the jacketing for about one meter from the base, as shown in Fig. 10.

Since the additional rebars were unconfined by stirrups and lateral buckling was only restrained by the adhesion of the HPFRC layer, the progressive deterioration of the bond between the jacketing and the substrate, as well as the plastic deformation of longitudinal reinforcements, can be identified as the main causes of buckling of the HPFRC layer that occurred when the drift was 3.4%. The extent of the unbonded area involved in the buckling failure was determined after the end of the test by the removal of the unbonded jacketing.

A noticeable reduction of deformation was observed in the strengthened specimen at SLS, with respect to the un-strengthened one, due to the increased stiffness provided by the HPFRC jacketing.

6. Concluding remarks

Based on the experimental study herein presented, the following conclusions can be drawn:

1. The effectiveness of a HPFRC jacketing as seismic retrofitting of a bridge pier was experimentally demonstrated. The jacketing was based on a 30 mm layer of self-compacting HPFRC applied on a sand-blasted existing pier; the addition of longitudinal steel reinforcements allowed a better connection of the jacketing to the foundation.
2. Although a very thin layer of jacketing was applied, the flexural capacity of the strengthened specimen increased more than 50% with respect to the un-strengthened specimen. Failure of the retrofitted pier was reached after yielding of the additional reinforcement with appreciable displacements, corresponding to a drift of 3.4%. However, a better detailing of the base section, with some confining rebars, would have provided additional bearing capacity and ductility to the element.
3. Lateral stiffness of the strengthened specimen was increased by

approximately 50% with respect to the elastic response of the un-strengthened element.

4. A diffused crack pattern with very small cracks (smaller than 0.2 mm at 1% drift) was observed on the surface of HPFRC jacketing.
5. The smaller crack opening, in addition to the very low porosity of the concrete matrix, are expected to significantly enhance the durability of the existing structure, thus providing a new and longer service life.

CRedit authorship contribution statement

Adriano Reggia: Conceptualization, Methodology, Software, Investigation, Writing - original draft, Writing - review & editing, Visualization. **Alessandro Morbi:** Conceptualization, Validation, Resources, Writing - review & editing, Project administration. **Giovanni A. Plizzari:** Conceptualization, Methodology, Writing - original draft, Writing - review & editing, Supervision, Project administration.

Declaration of Competing Interest

The authors declare that they have no known competing financial interests or personal relationships that could have appeared to influence the work reported in this paper.

Acknowledgements

The authors wish to express their gratitude and sincere appreciation to Italcementi HEIDELBERG Cement Group for financing this research work and other on-going research projects related to the innovative applications of High Performance Concrete. A special thanks to Eng. Mattia Ferrari, Eng. Luca Cominoli, Mr. Augusto Botturi, Mr. Domenico Caravaggi, Mr. Domenico Fiorillo, and Mr. Andrea Del Barba for their support in carrying out the experimental project.

References

- [1] Lee GC, Mohan SB, Huang C, Fard BN. A study of U.S. Bridge failures. MCEER Earthq Eng Extrem Events 2013.
- [2] Priestley MJN, Seible F, Calvi GM. Seismic design and retrofit of bridges. John Wiley & Sons; 1996.
- [3] Pinto AV, Molina J, Tsionis G. Cyclic tests on large-scale models of existing bridge piers with rectangular hollow cross-section. Earthq Eng Struct Dyn 2003. <https://doi.org/10.1002/eqe.311>.
- [4] Wang L, Su RKL, Cheng B, Li LZ, Wan L, Shan ZW. Seismic behavior of preloaded rectangular RC columns strengthened with precambered steel plates under high axial load ratios. Eng Struct 2017. <https://doi.org/10.1016/j.engstruct.2017.09.048>.
- [5] Parghi A, Alam MS. Seismic collapse assessment of non-seismically designed circular RC bridge piers retrofitted with FRP composites. Compos Struct 2017. <https://doi.org/10.1016/j.compstruct.2016.10.094>.
- [6] Unjoh S, Terayama T, Adachi Y, Hoshikuma J. Seismic retrofit of existing highway bridges in Japan. Cem Concr Compos 2000. [https://doi.org/10.1016/S0958-9465\(99\)00043-8](https://doi.org/10.1016/S0958-9465(99)00043-8).
- [7] Reggia A, Sgobba S, Macobatti F, Zanotti C, Minelli F, Plizzari GA. Strengthening of a bridge pier with HPC: Modeling of restrained shrinkage cracking. vol. 711. 2016. doi:10.4028/www.scientific.net/KEM.711.1027.

- [8] Cangiano S, Sgobba S. Comportamento meccanico e di durabilità del legame fra elementi strutturali in calcestruzzo e strati di UHPC e utilizzati per la riparazione ed il rinforzo, 2014.
- [9] Gholampour A, Hassanli R, Mills JE, Vincent T, Kunieda M. Experimental investigation of the performance of concrete columns strengthened with fiber reinforced concrete jacket. *Constr Build Mater* 2019. <https://doi.org/10.1016/j.conbuildmat.2018.10.236>.
- [10] Brühwiler E, Denarié E. Rehabilitation and strengthening of concrete structures using ultra-high performance fibre reinforced concrete. *Struct Eng Int J Int Assoc Bridg Struct Eng* 2013. <https://doi.org/10.2749/101686613X13627347100437>.
- [11] Schär P, Houriet B, Cuennet S, Fleury B, Mühlberg H, Bastien-Masse M, et al. Strengthening the Chillon viaducts deck slabs with reinforced UHPFRC. *IABSE Symp Rep* 2016. <https://doi.org/10.2749/222137815818358457>.
- [12] Brühwiler Eugen, Denarié Emmanuel. Rehabilitation of concrete structures using ultra-high performance fibre reinforced concrete. *UHPC-2008 Second Int Symp Ultra High Perform Concr* 2008.
- [13] Ilki A, Demir C, Bedirhanoglu I, Kumbasar N. Seismic retrofit of brittle and low strength RC columns using fiber reinforced polymer and cementitious composites. *Adv Struct Eng* 2009. <https://doi.org/10.1260/136943309788708356>.
- [14] Meda A, Mostosi S, Rinaldi Z, Riva P. Corroded RC columns repair and strengthening with high performance fiber reinforced concrete jacket. *Mater Struct Constr* 2016. <https://doi.org/10.1617/s11527-015-0627-1>.
- [15] Marini A, Meda A. Retrofitting of R/C shear walls by means of high performance jackets. *Eng Struct* 2009. <https://doi.org/10.1016/j.engstruct.2009.08.005>.
- [16] Cho CG, Han BC, Lim SC, Morii N, Kim JW. Strengthening of reinforced concrete columns by high-performance fiber-reinforced cementitious composite (HPFRC) sprayed mortar with strengthening bars. *Compos Struct* 2018. <https://doi.org/10.1016/j.compstruct.2018.05.045>.
- [17] Dagenais M-A, Massicotte B, Boucher-Proulx G. Seismic retrofitting of rectangular bridge piers with deficient lap splices using ultrahigh-performance fiber-reinforced concrete. *J Bridg Eng* 2017;23:4017129.
- [18] Reggia A, Sgobba S, Macobatti F, Zanotti C, Minelli F, Plizzari GA. Strengthening of a bridge pier with HPC: Modeling of restrained shrinkage cracking. *Key Eng Mater* 2016. <https://doi.org/10.4028/www.scientific.net/KEM.711.1027>.
- [19] Walvaren J. *Model Code 2010*, final drafts. *FIB Bull* 2012.
- [20] Paulay T, Priestley MJN. *Seismic design of reinforced concrete and masonry buildings* 1992.